ARTICLE IN PRESS

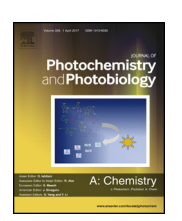
Journal of Photochemistry and Photobiology A: Chemistry xxx (2017) xxx-xxx



Contents lists available at ScienceDirect

Journal of Photochemistry and Photobiology A: Chemistry

journal homepage: www.elsevier.com/locate/jphotochem



Invited paper

Photocatalytic CO₂ reduction using water as an electron donor over Ag-loaded metal oxide photocatalysts consisting of several polyhedra of Ti⁴⁺, Zr⁴⁺, and Ta⁵⁺

Tomoaki Takayama^a, Haruka Nakanishi^a, Motoki Matsui^a, Akihide Iwase^{a,b}, Akihiko Kudo^{a,b,*}

^a Department of Applied Chemistry, Faculty of Science, Tokyo University of Science, 1-3 Kagurazaka, Shinjuku-ku, Tokyo, 162-8601, Japan

ARTICLE INFO

Article history: Received 20 August 2017 Received in revised form 27 September 2017 Accepted 1 October 2017 Available online xxx

Keywords: Heterogeneous photocatalyst CO₂ reduction Artificial photosynthesis

ABSTRACT

LaTa₇O₁₉ (BG: 4.1 eV) and CaTa₄O₁₁ (BG: 4.5 eV) with laminated structures consisting of layers of TaO₆ octahedra and TaO₇ decahedra were active for CO₂ reduction to form CO using water as an electron donor when an Ag cocatalyst of an efficient CO₂ reduction site was loaded. In contrast, the activity for the CO₂ reduction of CaZrTi₂O₇ (BG: 3.6 eV) with an anion-defect-type fluorite structure consisting of TiO₄ tetrahedra, TiO₆ octahedra, and ZrO₇ decahedra was negligible even when the Ag cocatalyst was introduced. Selectivity for the CO formation (CO/(H₂ + CO)) over the optimized Ag/LaTa₇O₁₉ photocatalyst reached around 95% in an aqueous NaHCO₃ solution. The rate of CO formation gradually decreased with a reaction time accompanied by an increase in the rate of H₂ evolution. The results of scanning electron microscopy (SEM), diffuse reflectance spectroscopy (DRS), and X-ray photoelectron spectroscopy (XPS) revealed that aggregation of the Ag cocatalyst during the photocatalytic CO₂ reduction caused the decrease in the CO formation.

© 2017 Elsevier B.V. All rights reserved.

1. Introduction

Photocatalytic CO_2 reduction using water as an electron donor has been paid much attention because it is the reaction that converts photon energy to chemical energy. Furthermore, the reaction has potential for CO_2 fixation to produce raw materials such as CO in C1 chemistry [1,2]. A powdered photocatalyst system is advantageous for a large-scale application because of its simplicity.

A ZrO₂ photocatalyst possessing the ability to split water is active for CO₂ reduction using water as an electron donor without any cocatalysts, giving CO as a reduction product of CO₂, H₂ as a reduction product of water, and O₂ as an oxidation product of water. Moreover, the CO selectivity is enhanced by loading a Cu cocatalyst [3]. BaLa₄Ti₄O₁₅ [4], CaTiO₃ [5], ZnGa₂O₄/Ga₂O₃ [6,7], KMM'Ta₅O₁₅ (M and M'=Ca and Sr) [8–10], NaTaO₃-based

photocatalyst [11], SrO-modified Ta₂O₅ [12], and ZnTa₂O₆ [13], which are active for water splitting [8,14–17], show activity for CO formation by the selective CO₂ reduction even in an aqueous solution when a metallic Ag nanoparticle cocatalyst was loaded. The Ag nanoparticle can be a model cocatalyst for surveying photocatalysts for the CO₂ reduction at the present stage.

The ability of photocatalytic CO_2 reduction strongly depends on a conduction band level. The band structure of a photocatalyst is dominated by the element and the crystal structure. The major crystal structures of photocatalysts reported for the CO_2 reduction are perovskite and tungsten bronze structures as seen in NaTaO3, $CaTiO_3$, $BaLa_4Ti_4O_{15}$, and $KMM'Ta_5O_{15}$ (M and M' = Ca and Ca). The crystal structures are composed of Ca0 and Ca1 and Ca2 reduction to survey photocatalysts composed of various constituent elements and crystal structures in order to make the photocatalyst library fruitful.

In the present study, the authors have focused on $CaZrTi_2O_7$ (BG: 3.6 eV) [18], $LaTa_7O_{19}$ (BG: 4.1 eV) [19], and $CaTa_4O_{11}$ (BG: 4.6 eV) [20] photocatalysts that have the ability to split water and unique crystal structures composed of MO_7 (M=Zr and Ta) decahedra and TiO_4 tetrahedra in addition to $M'O_6$ (M'=Ti and

https://doi.org/10.1016/j.jphotochem.2017.10.002 1010-6030/© 2017 Elsevier B.V. All rights reserved.

Please cite this article in press as: T. Takayama, et al., Photocatalytic CO₂ reduction using water as an electron donor over Ag-loaded metal oxide photocatalysts consisting of several polyhedra of Ti⁴⁺, Zr⁴⁺, and Ta⁵⁺, J. Photochem. Photobiol. A: Chem. (2017), https://doi.org/10.1016/j.jphotochem.2017.10.002

^b Photocatalysis International Research Center, Research Institute for Science and Technology, Tokyo University of Science, 2641 Yamazaki, Noda-shi, Chiba, 278-8510, Japan

^{*} Corresponding author at: Department of Applied Chemistry, Faculty of Science, Tokyo University of Science, 1-3 Kagurazaka, Shinjuku-ku, Tokyo, 162-8601, Japan. E-mail address: a-kudo@rs.kagu.tus.ac.jp (A. Kudo).

T. Takayama et al./Journal of Photochemistry and Photobiology A: Chemistry xxx (2017) xxx-xxx

Ta) octahedra being different from perovskite and tungsten bronze structures. CaZrTi₂O₇ has an anion-defect-type fluorite structure with TiO₄ tetrahedra, TiO₆ octahedra, and ZrO₇ decahedra (Fig. S1) [21]. LaTa₇O₁₉ and CaTa₄O₁₁ have laminated anisotropic structures consisting of layers of TaO₆ octahedra and TaO₇ decahedra (Figs. S2 and S3) [22,23]. Assuming the levels of valence band maxima formed by O 2p orbitals are +3.0 V vs. NHE at pH0 [15], the levels of conduction band minima estimated from those band gaps are quite negative compared with the potential to reduce CO_2 to CO(-0.12 V)vs. NHE at pH0). In other words, those band structures, which are composed of Ti 3d, Zr 4d, and Ta 5d orbitals to form the conduction bands and O 2p orbitals to form the valence bands, are thermodynamically preferable for CO₂ reduction to form CO accompanied by extraction of electrons from water. Therefore, these three metal oxides motivate us to evaluate those photocatalytic performances for the CO₂ reduction and examine what the main factor affecting those performances is.

In the present study, effects of loading the Ag cocatalyst on photocatalytic performances of $CaZrTi_2O_7$, $LaTa_7O_{19}$, and $CaTa_4O_{11}$ for CO_2 reduction were examined and the relationship between the band structures and the photocatalytic performances was discussed. Additionally, conditions of the Ag cocatalyst were investigated by SEM, DRS, and XPS.

2. Experimental

Amorphous precursors of CaZrTi₂O₇, LaTa₇O₁₉, and CaTa₄O₁₁ photocatalysts were prepared by a polymerized complex method according to the literatures [18–20]. The precursor of CaZrTi₂O₇ was calcined with Cs₂CO₃ of a flux reagent at 1273 K in air to obtain a nanocrystalline CaZrTi₂O₇ photocatalyst [18]. The obtained photocatalyst was washed with water to remove the flux reagent. The precursors of LaTa₇O₁₉ and CaTa₄O₁₁ were calcined at 1273 K and 1373 K in air, respectively [19,20]. The obtained samples were identified to be almost single-phase photocatalysts by X-ray diffraction patterns (XRD: Rigaku; MiniFlex (Cu $K\alpha$)) and diffuse reflectance spectra (DRS: Jasco; V-570) (Figs. S4-S6). The reflectance was converted to absorption using Kubelka-Munk function. An Ag cocatalyst was loaded on the surface of the obtained photocatalysts by photodeposition in situ, liquid-phase reduction [4], and impregnation. AgNO₃ was employed as the Ag cocatalyst source. Photodeposition was conducted in situ at the beginning stage of a photocatalytic reaction. In the impregnation, photocatalyst powder was dispersed in an aqueous AgNO₃ solution in a porcelain crucible. The slurry solution was stirred with a glass rod during evaporation using a hot plate. Obtained powder was calcined in air at 723 K for 1 h. In the liquid-phase reduction [4], an aqueous AgNO3 solution was added to an aqueous suspension containing of the photocatalyst. After addition of an equimolar amount of NaPH₂O₂ with respect to Ag $^{+}$ to the suspension, the mixture was stirred at 333 K for 1 h. The obtained powder was washed with water and dried at ambient temperature in air. The Ag cocatalyst was characterized using scanning electron microscopy (SEM: JEOL; JSM-7600F), DRS, and X-ray photoelectron spectroscopy (XPS: JEOL; JPS-9010MC, Mg anode). The binding energy of powder samples was corrected using a binding energy of C 1s of contamination (284.3 eV) on Au foil. The binding energy of the Au foil was corrected using the reference datum of Au foil (Au $4f_{7/2}$: 84.0 eV) [24] after contamination on the surface of the Au foil was carefully removed by Ar etching.

Photocatalytic CO₂ reduction and water splitting were conducted using a gas-flow system equipped with an inner irradiation quartz cell and a 400 W high-pressure mercury lamp. Photocatalysts were dispersed in water. NaHCO₃ was added into the aqueous solution, if necessary. CO₂ or Ar gas was continually bubbled into the aqueous suspension. The amounts of gaseous products were determined by gas-chromatographs (Shimadzu, GC-8A; TCD, MS-5A, Ar carrier; FID, MS-13X, a methanizer, N₂ carrier). An isotope experiment was conducted using ¹³CO₂ gas (99.5 atom %). The product of ¹³CO was analyzed using a GC-MS (Shimadzu; GC-MS Plus, RESTEK; RT-Msieve 5A).

3. Results and discussion

Table 1 shows CO₂ reduction in an aqueous solution with/ without NaHCO3 over LaTa7O19, CaTa4O11, and CaZrTi2O7 photocatalysts loaded with an Ag cocatalyst. CO formation over Agloaded LaTa₇O₁₉ (Ag/LaTa₇O₁₉) was observed. The CO formation hardly depended on the loading methods of the Ag cocatalyst regardless of the presence or absence of NaHCO3. It has been reported that the rate of CO formation over metal oxide photocatalysts loaded with the Ag cocatalyst decreases with an increase in the particle size of the Ag cocatalyst [4-13]. Since the Ag cocatalyst aggregated immediately during the CO₂ reduction even if the initial particle size of the Ag cocatalyst depended on the loading methods as mentioned later, the rate of the CO formation was insensitive to the initial condition of the Ag cocatalyst loaded by different methods. An impregnation method was slightly superior to liquid-phase reduction and photodeposition in situ regardless in the presence or absence of NaHCO₃. When NaHCO₃ was added into the reactant solution, Ag/LaTa7O19 prepared by impregnation gave 74% of relatively high selectivity for the CO formation. Consequently, the impregnation method was employed for evaluation of photocatalytic performances of CaTa₄O₁₁ and CaZrTi₂O₇ loaded with the Ag cocatalyst in an aqueous NaHCO₃ solution. Ag/CaTa₄O₁₁ showed high activity for CO₂ reduction as

Table 1 Effects of loading methods of an Ag cocatalyst and addition of NaHCO₃ on photocatalytic CO₂ reduction over LaTa₇O₁₉, CaTa₄O₁₁, and CaZrTi₂O₇ photocatalysts.

Photocatalyst	Band gap /eV	Loading method	NaHCO ₃	Initial rate/ μ mol h $^{-1}$			e^-/h^+	Selectivity
				H ₂	02	СО		%
LaTa ₇ O ₁₉	4.1	PD	No	15	9	2	0.9	12
LaTa ₇ O ₁₉	4.1	PD	Yes	13	18	23	1.0	64
LaTa ₇ O ₁₉	4.1	LPR	No	22	10	2	1.2	8
LaTa ₇ O ₁₉	4.1	LPR	Yes	16	20	24	1.0	60
LaTa ₇ O ₁₉	4.1	IMP	No	16	9	3	1.1	16
LaTa ₇ O ₁₉	4.1	IMP	Yes	9	17	25	1.0	74
CaTa ₄ O ₁₁	4.5	IMP	Yes	31	30	35	1.1	53
CaZrTi ₂ O ₇	3.6	IMP	Yes	Trace	Trace	Trace	_	_

Photocatalyst: 0.5 g, Ag cocatalyst: 1 wt%, reactant solution: 360 mL of water and an aqueous NaHCO₃ solution (0.1 mol L⁻¹), system: a CO₂ flow system, reactor: an inner irradiation cell made of quartz, light source: a 400 W high-pressure mercury lamp. t: trace, LPR: liquid-phase reduction, IMP: impregnation, PD: photodeposition in situ. e^-/h^+ = [(The sum of the rates of H₂ and CO formations/ μ mol h^{-1}) x 2]/[(Rate of O₂ formation/ μ mol h^{-1}) x 4]. Selectivity% = (Rate of CO formation/ μ mol h^{-1})/(The sum of the rates of H₂ and CO formations/ μ mol h^{-1}) x 100. Band gaps were estimated form the onsets of those diffuse reflectance spectra (Figs. S4–S6).

2

Download English Version:

https://daneshyari.com/en/article/6492595

Download Persian Version:

https://daneshyari.com/article/6492595

<u>Daneshyari.com</u>